Capturing and labeling CO_2 in a jar: Mechanochemical ^{17}O-Enrichment and ssNMR study of Sodium and Potassium (bi)carbonate Salts

Austin Peach,[1,*] Nicolas Fabrègue,[1] Célia Erre,[1] Thomas-Xavier Métro,[1] David Gajan,[2] Frédéric Mentink-Vigier,[3] Faith Scott,[3] Julien Trébosc,[4] Florian Voron,[5] Nicolas Patris,[6] Christel Gervais,[7] Danielle Laurencin[1,*]

1. ICGM, Univ Montpellier, CNRS, ENSCM, Montpellier, France

2. CRMN Lyon, UMR 5082 (CNRS, ENS Lyon, Université Lyon 1), Villeurbanne, France

3. National High Magnetic Laboratory (NHMFL), Florida State University, Tallahassee, Florida, USA

4. Université de Lille, CNRS, INRAE, Centrale Lille, Université d'Artois FR2638−IMEC−Institut Michel Eugène Chevreul, Lille, France

5. OSU OREME, UAR 3282, Université de Montpellier, CNRS, IRD, INRAE, Montpellier - Sète, France

6. HydroSciences Montpellier, UMR 5151, CNRS, IRD, Université de Montpellier, Montpellier, France

7. LCMCP, UMR 7574, Sorbonne Université, CNRS, Paris, France

To whom correspondence should be addressed:

austin.peach@umontpellier.fr

danielle.laurencin@umontpellier.fr

Abstract

With the rapid increase in temperatures around the planet, the need to develop efficient means to reduce CO_2 emissions has become one of the greatest challenges of the scientific community. Many different strategies are being studied worldwide, one of which consists in trapping the gas into porous materials, either for its short- or long-term capture and storage, or its re-use for the production of value-added compounds. Yet, to further the development of such systems, there is a real need to fully understand their structure and properties, including at the molecular-level following the physisorption and/or chemisorption of CO_2 (which can lead to various species, including carbonate and bicarbonate ions). In this context, ^{17}O NMR naturally appears as the analytical tool of choice, because of its exquisite sensitivity to probe subtle differences in oxygen bonding environments. To date, it has scarcely been used, due to the very low natural abundance of ^{17}O (0.04%), and the absence of commercially available ^{17}O-labeled compounds adapted to such investigations (*e.g.*, ^{17}O-$CO_{2(g)}$, or ^{17}O-enriched Na- and K-(bi)carbonate salts, which can be readily transformed into CO_2). Herein, we demonstrate how, using mechanochemistry, it is possible to enrich with ^{17}O a variety of Na- and K- (bi)carbonate salts in a fast, economical, scalable, and user-friendly way. The high enrichment levels enabled recording the first high-resolution ^{17}O ssNMR spectra of these phases at different temperatures and magnetic fields. From these, the typical spectral signatures of (bi)carbonate ions could be obtained, showing their strong sensitivity to local dynamics. Lastly, we show how thanks to the selective ^{17}O-labeling, singular aspects of the reactivity of carbonates in materials can be unveiled using *in-situ* ^{17}O ssNMR. In the long run, it is expected that this work will open the way to more profound investigations of the structure and properties of carbon capture and storage systems, and, more generally speaking, of functional materials containing carbonates.

Introduction

With temperatures constantly rising around the planet, and climate disasters increasing in frequency and intensity, it is urgent to rapidly develop ways of mitigating the causes of global warming, and notably anthropogenic carbon dioxide (CO_2) emissions.[1,2] In this context, much research has been dedicated to developing sustainable technologies for substantially reducing the net flow of CO_2 in the atmosphere by capturing it directly at industrial sources, with the aim of storing it either permanently (*e.g.*, in underground basaltic reservoirs), or temporarily (*e.g.*, before conversion into value added chemicals). Several different materials and processes have been investigated for this purpose.[3,4] On one hand, solutions and sorbents involving amine functionalities have been studied for decades: they can react with CO_2 to form ammonium carbamates or (bi)carbonates. However, their toxicity, corrosivity, and/or limited stability and recyclability (due to their degradation at high temperatures) were demonstrated to be problematic.[5] On the other hand, the potential of mineral carbonation has also been widely studied, including at the industrial scale: it consists of injecting and sequestering CO_2 into "reactive" natural rocks, so that it transforms into carbonate minerals (*e.g.*, metal carbonates like calcite and dolomite).[3,6,7] Along the same line, it has been proposed to use simple metal oxides like CaO as CO_2 sorbents by formation of $CaCO_3$, with applications tested up to the pilot scale.[8] Last but not least, several other classes of materials and sorbents have been investigated for CO_2 capture,[9] including metal organic frameworks (MOFs),[10] which, depending on their structure, can incorporate CO_2 in their pores by physisorption and/or chemisorption.[11,12]

Although a large diversity of systems was studied and developed for CO_2 capture, several aspects of the reactivity of this small molecule still deserve to be answered to ensure the optimal design and understanding of hitherto carbon capture systems. Indeed, beyond the identification of the CO_2 speciation in the final material, which can involve either CO_2 molecules upon physisorption, or (bi)carbonate/carbamate ionic entities upon chemisorption, numerous points are still obscure. Among these, the questions of the impact of temperature, pressure, and moisture on the binding modes of CO_2, its speciation, and the local molecular motions it undergoes, still need to be investigated in detail, in view of helping conceive and improve, on the long run, the carbon-capture properties of these systems.

As a local analytical probe, NMR spectroscopy naturally appears as perfectly suited for studying CO_2 environments within carbon-capture materials, and it has already been used in numerous investigations.[13–15] To date, the vast majority of NMR studies have concerned

carbon-13,[15] due to the higher sensitivity of this spin-1/2 nucleus. Yet, oxygen-17, the only stable isotope of oxygen which can be analyzed by NMR, is also highly attractive: *(i)* its chemical shift range exceeds 1000 ppm (in comparison to only *ca*. 200 ppm for ^{13}C);[16] *(ii)* it has a spin-5/2 quadrupolar nucleus, meaning that complementary information on its local electronic environment can be derived from the quadrupolar parameters C_Q and η_Q (which is not the case for ^{13}C, as it is only spin-1/2); *(iii)* the ^{17}O lineshape is exquisitely sensitive to molecular-level dynamics, making variable-temperature ^{17}O NMR studies richly informative on local motions;[17–21] *(iv)* while only one ^{13}C resonance is expected per CO_2 molecule or (bi)carbonate/carbamate species attached to a surface, 2 (or 3) distinct ^{17}O resonances can potentially be observed, meaning that the latter can garner more detailed information on the bonding, reactivity, and adsorption modes of CO_2.

Despite all these advantages, to the best of our knowledge, ^{17}O NMR has only been used six times in the context of carbon-capture materials and systems: *(i)* to study CO_2 dynamics within MOF-74, looking at its ^{17}O NMR signature at different temperatures,[22] *(ii)* to investigate *in-situ* the dissolution of $Mg(OH)_2$ (brucite) in a water/supercritical CO_2 ($scCO_2$) fluid, in conditions relevant to geological carbon sequestration;[23] *(iii)* to identify the chemisorption mode of CO_2 in amine-functionalized sorbents (MOFs and mesoporous silica)[14] or *(iv)* hydroxide-based MOFs;[19] *(v)* to determine the adsorption site of CO_2 on MgO nanosheets,[19,24] and *(vi)* to help understand the exchange mechanism between atmospheric CO_2 and carbonate anions intercalated within layered double hydroxides.[25] In all cases, ^{17}O NMR spectroscopy provided clues on the structure and/or reactivity of the different systems. The dearth in the number of ^{17}O NMR studies of carbon-capture materials originates from the meagre natural abundance of ^{17}O (0.04%, compared to 1.1% for ^{13}C). Indeed, in the aforementioned examples, only one ^{17}O NMR study was fully performed at natural abundance (dissolution of brucite in $H_2O/scCO_2$ mixtures), which required using concentrated *solutions*, a large sample-volume NMR probe, and high magnetic fields (*i.e.*, 900 MHz instrument).[23] In the five other cases, ^{17}O NMR studies were performed in the *solid state*, implying much broader ^{17}O resonances due to the absence of complete averaging of the quadrupolar interaction. When performed at natural abundance, such ^{17}O solid-state (ssNMR) studies are highly challenging, as shown recently in the analysis of simple $KHCO_3$ and $K_2CO_3{\cdot}1.5H_2O$ phases: despite the lengthy acquisition times (15 to 42 h) at (ultra)-high magnetic fields (*i.e.*, 850 MHz and 1.0 GHz NMR instruments) poorly defined 1D lineshapes with a low signal-to-noise ratio were obtained,[19] from which ^{17}O NMR parameters could not be extracted unambiguously nor with high accuracy (hence making the spectral interpretations difficult). This is why most of the aforementioned ^{17}O ssNMR

analyses were carried out on *isotopically enriched* species, with the initial ^{17}O-labeling either on the CO_2 gas,[14,19,22] the material of interest,[24] or the surrounding medium (H_2O).[25] Yet, with limited ^{17}O-enriched precursors commercially available (the main two being ^{17}O-enriched water and ^{17}O-O_2 gas), and with only one supplier actually willing to produce and sell ^{17}O-enriched CO_2 gas (but with constraints and delays for its delivery to academic laboratories, because the product is classified as a "dangerous goods" for transportation),[a] any prospect of a widespread application of ^{17}O ssNMR for the engineering of materials and sorbents for CO_2 capture appears restricted.

Spurred by this general context, we decided to focus on developing efficient and cost-effective routes for enriching in ^{17}O carbonate and bicarbonate salts of sodium (*i.e.*, $Na_2CO_3{\cdot}H_2O$, Na_2CO_3 and $NaHCO_3$), and potassium (*i.e.*, $K_2CO_3{\cdot}1.5H_2O$ and $KHCO_3$). Indeed, three key advantages can be seen in being able to enrich these compounds. First, they are known to decompose upon heat treatment or acidic exposure by releasing CO_2, which makes them attractive sources for the production of ^{17}O-enriched CO_2 for further studies of its capture by different sorbents. Second, they encompass a variety of local environments for (bi)carbonate ions, which can be representative of those expected to be found within materials developed for carbon capture. Thus, performing *high-resolution* ^{17}O ssNMR studies on these phases is necessary for establishing key aspects regarding their spectral signatures within solids, as this is crucial to be able to derive sound conclusions on the structure and dynamics of CO_2-related species within more complex materials. Last, beyond CO_2-capture applications, Na- and K-(bi)carbonates are actually key precursors used for the synthesis of many different types of (bio)materials, meaning that their ^{17}O enrichment could also be valuable to the investigation of a much broader diversity of materials and systems.

In this manuscript, we will first demonstrate how, using mechanochemistry, it is possible to enrich the aforementioned Na- and K- (bi)carbonate salts in ^{17}O, in a highly efficient way. Then, the high-resolution ^{17}O ssNMR spectra of the isotopically-enriched compounds will be presented, revealing their strong dependency to the local structure and dynamics around the (bi)carbonates. Finally, we will show how thanks to the high ^{17}O-enrichment, singularities about the reactivity of carbonates in materials can be brought to light through *in-situ* ^{17}O ssNMR analyses, which will help open the way to more profound investigations of the properties of carbon capture systems, and, more generally, of functional materials containing carbonates.

[a] Request for a quote for ^{17}O-enriched CO_2 was made in July/August 2024 to 7 different suppliers (for which the websites mentioned the possibility to order ^{17}O-enriched CO_2). Only one positive answer was received, with constraints and delays for its delivery.

1. Experimental details

1.1 Materials

Carbonyldiimidazole (CDI, TCI, >97% purity) was used as received. Due to its sensitivity to air and humidity, it was systematically stored under Argon and in a fridge. Its purity (lack of hydrolysis) was regularly checked by IR spectroscopy, by verifying the absence of imidazole vibration bands. If impure, a new jar was ordered immediately.

Sodium hydroxide pellets (NaOH, Acros Organics, 98% purity) or micropearls (NaOH, Chem-Lab, 98.5+% purity), and potassium hydroxide pellets (KOH, Sigma-Aldrich, 85% purity), were used as received. These reagents were analyzed by IR and pXRD, revealing the presence of water and carbonate impurities. In the case of NaOH, a more significant hydration was noticed for the micropearls, which explains why this reagent had to be introduced in larger excess in the reactions described below. NaOH educts were stored under air, while KOH, which is more hygroscopic, was stored under Ar.

Labeled water was purchased from Cortecnet or Eurisotop, and used as received. The isotopic compositions provided in the certificates of analysis were as follows:

- $H_2{}^{18}O$ with 99% enrichment (composition: 0.1% ^{17}O, 99.5% ^{18}O, 0.4% ^{16}O), and
- $H_2{}^{17}O$ with 40% (composition: 39.30% ^{17}O, 44.6% ^{18}O, 16.10% ^{16}O), 70% (composition: 70.37% ^{17}O, 3.29% ^{18}O, 26.34% ^{16}O), or 90% enrichment (composition: 91.0% ^{17}O, 1.0% ^{18}O, 8.0% ^{16}O).

1.2 Mechanochemical Syntheses

A Retsch Mixer Mill 400 (MM400) was used for the mechanochemical syntheses, with the general reaction shown in **Figure 1B**. All reactions were performed in 10 mL stainless steel jars with two stainless steel ball bearings (10 mm in diameter), and the joint of the jar was sealed with parafilm during the milling. After milling, the jar was opened and the completion of the reaction was immediately verified by IR.

Reactions were first tested and optimized using ultra-pure water, prior to using ^{18}O- and ^{17}O-labeled water. We note that the order of the reagents described below is critical as CDI reacts rapidly with H_2O to form CO_2. Thus, to minimize the interaction of these educts before the milling, the balls were introduced immediately after the water (to “cover” the water and

occupy more space in the jar), followed by MOH, and CDI was introduced last. The jar was then sealed as fast as possible (to avoid "losing" any CO_2).

In terms of stoichiometries, a 2:1 molar ratio between H_2O and CDI was systematically used (implying a small excess in H_2O), while the amount of base (NaOH or KOH) was adapted case by case, to enable formation of pure bicarbonate or carbonate salts (see electronic supporting information (ESI) **Supplementary Information S1** for further details).

The texture of the product after grinding was found to vary depending on the synthesis and volume of water used, making the crude sample more or less easy to recover. During the work-up, the nature and quantity of absolute EtOH was adapted such that the imidazole by-product was fully removed, while the majority of (bi)carbonate salt was kept. Drying was performed to remove any excess solvent and potential residual water. Once isolated, the samples which had been synthesized using enriched water were stored under argon gas and placed in a fridge.

Details pertaining to the synthesis of sodium (Na) and potassium (K) (bi)carbonates are found below, with examples of the typical masses of educts and products reported in **Table 1**.

$Na_2CO_3 \cdot H_2O$ and Na_2CO_3

H_2O (2 eqv.), NaOH micropearls (2.6 eqv.), and CDI (1 eqv.) were introduced successively into the milling jar in the following order alongside the stainless steel ball bearings: *(i)* H_2O, *(ii)* two 10 mm balls, *(iii)* NaOH, and *(iv)* CDI. The jar was quickly closed, sealed, and the medium milled for 30 minutes at 25 Hz. After milling, the jar was opened and the white paste was scraped using a spatula and transferred on a P4 frit, trying to recover the majority of the product. The rest was recovered with a pipette, by adding absolute EtOH in small fractions to the jar (5 mL in total), which were then added onto the glass frit. The wet precipitate was filtered under dynamic vacuum and washed 3 times with 5 mL of EtOH, followed by 2 x 5 mL Et_2O. The product was left to dry under vacuum for 1 hour. Once dry, the white solid was scraped from the frit onto aluminum foil and transferred to a vial. Average synthetic yield (n = 3): 87 ± 5 %. Typical amount isolated (for quantities in **Table 1**): *ca.* 120 mg.

To obtain anhydrous Na_2CO_3, the monohydrate salt was transferred into a vial, and a heat treatment was performed at 100°C during *ca.* 3 hours in an oven under air. Average synthetic yield (n = 3): 90 ± 7 %. Typical amount isolated (when heat-treating 75 mg of monohydrate): *ca.* 60 mg.

$NaHCO_3$

H_2O (2 eqv.), NaOH pellets (0.5 eqv.), and CDI (1 eqv.) were introduced successively into the milling jar in the following order alongside the stainless steel ball bearings: *(i)* H_2O, *(ii)* two 10 mm balls, *(iii)* NaOH, and *(iv)* CDI. The jar was quickly closed, sealed, and the medium milled for 30 minutes at 25 Hz. After milling, the jar was opened and then the wet paste was scraped using a spatula to recover the majority of the product on a P4 frit. The rest was recovered with a pipette, by adding absolute EtOH in small fractions to the jar (5 mL in total), which were then added onto the glass frit. The wet precipitate was filtered under dynamic vacuum, and washed 3 times with 5 mL of EtOH, followed by 2 x 5 mL Et_2O. The product was left to dry under vacuum for ca.1 hour. Once dry, the white solid product was scraped from the frit onto aluminum foil and transferred to a vial. Average synthetic yield (n = 6): 84 ± 7 %. Typical amount isolated (for quantities in **Table 1**): *ca.* 80 mg.

$K_2CO_3 \cdot 1.5H_2O$

H_2O (2 eqv.), KOH (2 eqv.), and CDI (1 eqv.) were introduced successively into the milling jar in the following order, alongside the stainless steel ball bearings: *(i)* H_2O, *(ii)* two 10 mm balls, *(iii)* KOH, and *(iv)* CDI. The jar was quickly closed, sealed, and the medium milled for 30 minutes at 25 Hz. After milling, the jar was opened and the sample appeared as a white solid. The contents were scraped using a spatula and transferred onto a P4 frit. Using a pipette, 5 x 1 mL fractions of absolute EtOH were then used to rinse and recover any remaining precipitate in the jar and added to the P4 frit. The wet precipitate on the glass frit is then washed with 5 x 1 mL fractions of Et_2O. The product was left to dry under dynamic vacuum for 30 minutes. Once dry, the white solid product was scraped from the frit onto aluminum foil, and then transferred to a vial. Average synthetic yield (n = 3): 61 ± 6 %. Typical amount isolated (for quantities in **Table 1**): *ca.* 80 mg.

$KHCO_3$

H_2O (2 eqv.), KOH (0.5 eqv.), and CDI (1 eqv.) were introduced successively into the milling jar in the following order, alongside the stainless steel ball bearings: *(i)* H_2O, *(ii)* two 10 mm balls, *(iii)* KOH, and *(iv)* CDI. The jar was quickly closed, sealed, and the medium milled for 30 minutes at 25 Hz. After milling, the jar was opened and the sample appeared as a white paste. The contents were scraped using a spatula and transferred onto a P4 frit. Using a

pipette, 5 x 1 mL fractions of absolute EtOH were used to rinse and recover any remaining precipitate from the jar, and added to the P4 frit. The wet precipitate on the glass frit was then washed with 5 x 1 mL fractions of Et_2O. The wet product was left to dry under dynamic vacuum for 30 minutes. Once dry, the white solid product was scraped from the frit onto aluminum foil and transferred to a vial. Average synthetic yield (n = 3): 67 ± 6 %. Typical amount isolated (for quantities in **Table 1**): *ca.* 115 mg.

1.3 Characterizations

Attenuated Total Reflectance Infra Red spectroscopy

Attenuated total reflectance IR (ATR-IR) analyses were performed either using a Perkin Elmer Spectrum 2 instrument in a range of 400 to 4000 cm^{-1}, or using a Perkin Elmer Spectrum 100 instrument in the range of 650 to 4000 cm^{-1}. Depending on the instrument, 4 or 8 scans were acquired for both the background and sample. IR was used to monitor the course of the reactions, assess the purity of educts and products, and have a first evaluation of the successful enrichment of the final products.

Powder X-ray Diffraction

A Malvern PANalytical X'Pert MPD diffractometer (1.5406 Å Cu Kα wavelength, 40kV and 25 mA) was used to acquire powder X-ray diffraction (pXRD) patterns. Samples were placed onto glass plates, and analyzed in a diffraction range of 5° or 10° to 70° 2θ using a step size of 0.033°, with experimental times of *ca.* 8 to 10 minutes. pXRD was used to assess the purity and crystallinity of the final products, by comparison to reference powder patterns of Na- and K- (bi)carbonates.

Isotope Ratio Mass Spectrometry analyses of Na-carbonate Salts

Isotopic abundances of ^{16}O and ^{18}O in Na-carbonate salts were determined by isotope ratio mass spectrometry (IRMS). Samples were analyzed on a KIEL IV Carbonates apparatus (ThermoFisher Scientific), connected to a Delta V+ Dual Inlet mass spectrometer (ThermoFisher Scientific) of the AETE-ISO analytical platform (OREME, Montpellier, France). Controls of the isotopic ^{18}O enrichment of water were performed by CRDS Laser spectroscopy on a Picarro L2130-i analyzer at the LAMA laboratory of Hydrosciences

Montpellier, and were used to assess the reaction yields. Further information regarding the precise analysis conditions and accompanying enrichment calculations on the samples (and labeled waters used for their synthesis) are provided in the ESI, as part of **Supplementary Information S2**. The measured ^{18}O contents are grouped in **Table S1.**

^{13}C Solid-State NMR

^{13}C solid-state NMR (ssNMR) magic angle spinning (MAS) spectra were recorded at 14.1 T [$\nu_0(^1H)$ = 599.765 MHz and $\nu_0(^{13}C)$ = 150.810 MHz] (600 MHz instrument) on a Varian VNMRS spectrometer using a 3.2 mm HXY probe with samples packed into 3.2 mm outer diameter (o.d.) zirconia pencil rotors. The sample temperatures are estimated to be 280 K. Most spectra were acquired using a ^1H-^{13}C variable-amplitude cross polarization (VACP)[26] sequence at a spinning rate of ν_{rot} = 10 to 12 kHz, with SPINAL-64[27,28] ^1H decoupling during acquisition (50 kHz RF). Only the ^{13}C NMR spectrum of Na_2CO_3 was acquired using a direct excitation (one pulse) experiment. Further experimental acquisition parameters can be found in **Table S2**. All ^{13}C chemical shifts were referenced to adamantane (high frequency peak at δ_{iso} = 38.5 ppm with respect to neat TMS).

^{17}O Solid-State NMR

^{17}O ssNMR 1D and 2D MAS spectra were recorded at various NMR facilities (*i.e.*, ICGM in Montpellier, IMEC University of Lille in Villeneuve d'Ascq, CRMN Lyon in Villeurbanne, and NHMFL in Tallahassee), using different magnetic fields (B_0 = 14.1 T, 18.8 T, and 28.2 T), and measurement temperatures (between *ca.* 105 K and 365 K). General details regarding the field, facility, and accompanying experiments can be found below, while the sample temperatures and acquisition parameters are summarized in the ESI **Tables S3 to S7**. A double frequency sweep (DFS) was applied to enhance the sensitivity of ^{17}O MAS spectra by a factor of *ca*. 2 to 3 fold.[29] For samples containing protons, SPINAL-64 ^1H decoupling was applied during acquisition, using a radio frequency of 75 kHz to 100 kHz.[27,28] ,

Experiments at 14.1 T were conducted at the ICGM (Montpellier, France) and the National High Magnetic Field Lab (NHMFL, Tallahassee, Florida). At ICGM [$\nu_0(^1H)$ = 599.765 MHz, $\nu_0(^{17}O)$ = 81.307 MHz], ^{17}O NMR spectra were recorded on a Varian VNMRS spectrometer using a 3.2 mm triple-resonance HXY Varian probe with samples packed into 3.2 mm o.d. zirconia rotors with Torlon drive tips and caps. Samples were spun at

a rate of ν_{rot} =16 kHz or 20 kHz with the sample temperatures estimated to be between 240 to 370 K, and spectra were acquired using a one pulse or DFS enhanced Hahn echo pulse sequence with a π/2 solid pulse of 2 μs, followed by a 4 μs π pulse, and using an echo delay of one rotor period. At NHMFL [$\nu_0(^1H)$ = 600.486 MHz, $\nu_0(^{17}O)$ = 81.405 MHz], ^{17}O NMR spectra were recorded on a Bruker Avance NEO spectrometer using a custom-built low-temperature 3.2 mm HXY MAS-DNP probe with samples packed into sapphire rotors with Vespel drive caps. Samples were spun at a rate of ν_{rot} = 10 or 11 kHz at *ca*. 105 K, and spectra were acquired using similar acquisition conditions as at higher temperature.^{17}O chemical shifts were referenced directly to tap water at 0 ppm.[b]

Experiments at 18.8 T [$\nu_0(^1H)$ = 799.700 MHz, $\nu_0(^{17}O)$ = 108.411 MHz] were conducted at the CRMN Lyon (Villeurbanne, France). ^{17}O NMR spectra were recorded on an Avance NEO spectrometer using a 3.2 mm triple-resonance HXY ultra-low temperature DNP Bruker probe, with samples packed into 3.2 mm o.d. zirconia rotors with Vespel drive tips, using a spinning rate of ν_{rot} = 12.5 kHz, and regulating near room temperature. Spectra were acquired using either a DFS-enhanced Bloch decay (one pulse) or Hahn echo pulse sequence with a π/2 solid pulse of 2.8 μs (followed in the case of the echo by a π pulse of 5.6 μs with an echo delay of one rotor period), both with and without ^1H decoupling. ^{17}O chemical shifts were referenced directly to tap water at 0 ppm.[b]

Experiments at 28.2 T [$\nu_0(^1H)$ = 1200.540 MHz; $\nu_0(^{17}O)$ = 162.751 MHz] were conducted at the IMEC (Villeneuve d'Ascq, France). ^{17}O NMR spectra were recorded on an Avance NEO spectrometer using a 1.3 mm double-resonance HX Bruker probe with samples packed into 1.3 mm o.d. zirconia rotors with Vespel drive tips, using a spinning rate of ν_{rot} = 50 kHz, and regulating the temperature at c*a*. 250 K. All spectra were acquired using a DFS enhancement. 1D Bloch decay (one pulse) or echo pulse sequences were recorded with a π/2 solid pulse of 6 μs, followed by a 12 μs π pulse for echo experiments. 2D ^1H-^{17}O dipolar mediated heteronuclear multiple-quantum coherence (D-HMQC) and dipolar driven insensitive nuclei enhanced by polarization transfer (D-INEPT) spectra were acquired using the $SR4_1^2$ (270_090_{180})[30] recoupling scheme with a π/2 pulse of 6 μs and 1.4 μs on ^{17}O and ^1H, respectively, with the total recoupling time varied from 100 μs to 1000 μs. Spectra were equivalently referenced to match H_2O at 0 ppm.[c,31]

[b] The ^{17}O NMR spectrum of D_2O was recorded, and found to be shifted by *ca*. -2.7 ppm compared to tap water.
[c] The « universal referencing » procedure was used for referencing the ^{17}O NMR spectra recorded at 28.2 T. First, the ^1H chemical shift of adamantane was set to δ_{iso} = 1.74 ppm (secondary reference with respect to TMS in

All spectra were processed using the TopSpin v4.1.4 and ssnake v1.5[32] software packages. All analytical simulations of the ^{17}O NMR parameters were obtained using the quadrupolar fitting module included in ssnake with the uncertainties assessed by bidirectional variation of each parameter. In the figures below, the actual sample temperatures are provided; these were calibrated using KBr.[33] The chemical shift scales are given both in ppm and kHz, to highlight the breadth of the signals according to both units.

1.4 Computational Details

Geometry optimizations on the reported crystal structures of Na- and K- (bi)carbonate salts[34–38] were carried out using the Vienna *ab initio* simulation package (VASP)[39–41]. The revised Perdew-Burke-Erzenhof (rPBE)[42] generalized gradient approximation (GGA) functional was used, with an energy cut-off of 400 eV, a Monkhorst-Pack k-space grid size chosen to obtain a unit cell with cubic symmetry, and employing Grimmes D3 dispersion correction.[43] All atom (All Rel) positions were optimized, while keeping the unit cell fixed.

Subsequent NMR calculations of the NMR parameters, the electric field gradient (EFG) tensor parameters (*i.e.*, C_Q and η_Q) and chemical shieldings (σ_{calc}) were performed on VASP geometry optimized structural models, using plane-wave density functional theory (DFT), as implemented in the QUANTUM-ESPRESSO (QE) software.[44] The NMR parameters were computed using the GIPAW approach,[45] with the PBE[46] GGA functional, norm conserving pseudopotentials in the Kleinman-Bylander form to describe the valence electrons,[47] an energy cut-off of 80 Ry, and a k-space grid as reported in supporting information (**Table S8**).

The calculated ^{17}O NMR parameters for fully-relaxed structural models of Na- and K-(bi)carbonates are provided in **Table S8**. The quadrupolar moment of –2.558 fm^2 was used for the calculation of the ^{17}O quadrupolar coupling constants (C_Q).[48] The ^{17}O isotropic chemical shifts δ_{iso} were estimated from the calculated isotropic shieldings σ_{iso}, using, as a first approximation, the following equation: $\delta_{iso} \approx -(\sigma_{iso} - \sigma_{ref})$. Here, a σ_{ref} value of 228 ppm was used, as in a recent publication.[49] Structures and further computational details are available upon request.

$CDCl_3$). Then, the reference frequency for neat D_2O at δ_{iso} = 0.00 ppm was calculated using the IUPAC factor Ξ = 13.556457 (see ref. 31). Finally, ^{17}O NMR chemical shifts were back-corrected by 4.3 ppm, because non-labeled H_2O had been measured experimentally at 4.3 ppm at the IMEC, after calibration using this procedure).

2. Results and Discussion

2.1 Mechanochemical Isotopic Enrichment

To the best of our knowledge, two main synthetic approaches have been used so far in the literature for the ^{17}O-labeling of carbonate salts for ssNMR (**Figure 1A**): *(i)* the equilibration of carbonate ions in the presence of labeled water (to eventually form enriched Ca- or mixed Ca, Mg-carbonates),[50,51] and *(ii)* the quantitative reaction of CO_2 gas with pre-labeled LiOH (to form enriched Li_2CO_3).[18,52] In the former case, long reaction times (*ca*. 1 week at 90 °C)[50] and/or an excess of expensive ^{17}O-labeled water were used to ensure sufficient labeling. In the latter case, the synthesis was constraining, due to the high reactivity of the reagents (*n*-butyllithium in dry THF), and the need to manipulate CO_2 gas at 100 °C.[18,52] From what was reported, it appears that none of these procedures was optimized in terms of synthetic yields and ^{17}O-enrichment levels, and their scalability or transposability to the isolation of pure Na- and K- (bi)carbonate salts was not reported. Moreover, to our knowledge, none of these reaction protocols was widely adopted by synthetic chemists, further demonstrating the need to develop more efficient procedures in terms of time, cost, and practicality.

As an alternative synthetic approach, we looked into trying to enrich (bi)carbonate salts using mechanochemistry. Initial attempts were performed by simply milling the Na_2CO_3 precursor in presence of stoichiometric amounts of labeled water. Indeed, considering that mechanochemical reactions can help accelerate reaction kinetics between reagents, due to the highly concentrated conditions in the milling jar, we considered the possibility of performing a direct isotopic enrichment by an "equilibration" type of reaction under these conditions. These first tests were carried out with ^{18}O-enriched water (due to its *ca*. 30-fold lower cost compared to the ^{17}O-enriched water), and the milling was performed for 30-90 minutes on a horizontal mixer mill, with stainless steel jars and beads. The products recovered after milling were dried and analyzed by pXRD to confirm phase purity, followed by mass-spectrometry (MS) and/or IR spectroscopy to determine if ^{18}O-labeling had occurred. In all cases, no clear isotope-shift of the carbonate vibration bands could be observed by IR spectroscopy, suggesting that the labeling achieved (if any) was very low. Quantitative IRMS analyses on Na-carbonate salts confirmed that the maximum ^{18}O level achieved was less than 0.6% (when starting from 99% ^{18}O-enriched water), which corresponds to a mere 3-fold increase compared to the ^{18}O natural abundance (0.2%), and remains well beneath the maximum value of *ca*. 40% (calculated for a

full scrambling of the oxygen isotopes in the experimental conditions used - see **Supplementary Information S2**). Although prolonging milling times or increasing the amount of labeled water should help further enhance the labeling level, such experiments were not attempted, as they would decrease the attractiveness of the enrichment procedure (*i.e.*, due to the significantly-increased experimental times and/or higher costs for ^{17}O-labeling). Moreover, contaminations from the jar and beads would occur upon longer milling times, thereby simultaneously implying a loss in purity of the final product.

A second synthetic approach was thus considered (**Figure 1B**), which consisted in performing a one-pot quantitative transformation by mechanochemistry. The general idea was to simultaneously introduce in the milling jar *N*,*N*′-carbonyl-diimidazole (CDI), ^{17}O-labeled water, and an alkali metal base (*e.g.*, NaOH or KOH), in order to hydrolyze the CDI precursor to form ^{17}O-labeled CO_2, and directly trap this gas with the base to form the desired (bi)carbonate salt. Initial tests were carried out with non-labeled water (to optimize the synthetic yield), before moving on to ^{18}O-enriched water (to estimate the enrichment level), and finally ^{17}O-enriched water (in view of ^{17}O NMR analyses). The amount of base was adapted to ensure the direct formation of either a bicarbonate or a carbonate salt in the jar. In all cases, full consumption of the NaOH (or KOH) and CDI precursors was observed after only 30 minutes of milling. This was attested by IR spectroscopy (see ESI, **Figures S1** to **S4**), through *(i)* the disappearance of the vibration bands characteristic of the reagents (especially the OH stretching band), and *(ii)* the appearance of the vibration bands of the products (especially the imidazole by-product). The latter was removed during a work-up step, by dissolution in an appropriate solvent. The final (bi)carbonate salts were dried, and subsequently characterized by powder X-ray diffraction (pXRD), IR spectroscopy, and ^{13}C solid state NMR, confirming the formation of phase-pure forms of $NaHCO_3$, $KHCO_3$, $Na_2CO_3{\cdot}H_2O$, and $K_2CO_3{\cdot}1.5H_2O$ (see ESI **Figures S5** to **S11**). A pure phase of anhydrous Na_2CO_3 was isolated by heat-treatment of $Na_2CO_3{\cdot}H_2O$ for a few hours at 100 °C.

Comparison of the IR spectra of samples prepared using non-labeled, ^{17}O-labeled, and ^{18}O-labeled water provided evidence of the success of the isotopic labeling of the (bi)carbonate ions. This is illustrated in **Figure 2**, in which some of the spectral regions where variations caused by ^{17}O or ^{18}O isotope shifts are highlighted. Notably, regarding the carbonate salts, the splittings at *ca*. 1065 cm^{-1} for $Na_2CO_3{\cdot}H_2O$ and $K_2CO_3{\cdot}1.5H_2O$ (ν_1 stretching mode), and at *ca*. 1775 cm^{-1} for Na_2CO_3 (tentatively assigned to the 2 × ν_2 harmonic)[53] show contributions from the different $C^{16}O_n{*}O_{3-n}^{2-}$ (n = 1, 2 and 3) isotopologues.[54–56] In the case of ^{18}O-labeled salts,

analyses of the relative intensities of the different bands enabled to estimate the ^{18}O enrichment level to be above 25% (when starting from 99% ^{18}O-labeled water). Further IRMS analyses on ^{18}O-labeled Na-carbonates were performed, confirming the quantitative ^{18}O-labeling of the carbonates when using CDI-based procedures (see **Supplementary Information S2**).

Overall, the CDI-strategy proposed is particularly efficient for the production of $^{17}O/^{18}O$-labeled Na- and K- (bi)carbonate salts, enabling to isolate phase-pure compounds in half a day (work-up included), with a high enrichment level. The protocols are robust and user friendly (performed under ambient temperature and pressure), and do not require the use of highly toxic reagents or constraining procedures (*vide supra*). Herein, syntheses are described in quantities enabling the isolation of up to *ca*. 130 mg of product (**Table 1**). Yet, reactions can be readily adapted to produce larger amounts of labeled products, by performing reactions simultaneously in two jars (when using a horizontal mixer mill), increasing the amount of sample per jar, and/or by using larger volume reactors. In the course of our investigations, by simply tripling the initial amount of reagents, we were able to produce 400 mg of ^{17}O-enriched Na_2CO_3 in just half a day. This makes CDI-based $^{17}O/^{18}O$-labeling far more promising than the previously described labeling schemes (**Figure 1A**), and thus highly attractive for pushing forward ^{17}O ssNMR studies on materials containing (bi)carbonate-related species.

2.2 High-resolution ^{17}O ssNMR of ^{17}O-labeled sodium and potassium (bi)carbonates

The ^{17}O ssNMR spectra of the five Na- and K- (bi)carbonate salts were first acquired at 14.1 T (*i.e.*, 600 MHz instrument) using standard analytical conditions (MAS analyses at moderate spinning speed and sample temperatures *ca*. 263 K to 270 K). In all cases, the successful enrichment enabled the observation of a ^{17}O NMR signal in just one scan, with experiments shown in **Figure 3A** taking as little as 30 minutes in the best case (see **Table S3** for experimental details). This is a significant improvement in comparison to a recently reported work, where the naturally abundant spectra of the two K salts (*i.e.*, $KHCO_3$ and $K_2CO_3{\cdot}1.5H_2O$) required more than one day to acquire on a higher magnetic field instrument (23.5 T field, *i.e.*, 1 GHz instrument).[19]

^{17}O NMR signals were observed in two key spectral regions, located in the following shift ranges (at 14.1 T): *(i)* between 200 and 40 ppm for *all* Na- and K- (bi)carbonate salts

(**Figure 3A**, orange zone), which is in the zone expected for carbonate-like environments;[18,19,25,50,57] and *(ii)* between 0 and −120 ppm for the two hydrates (**Figure 3A**, blue zone), which corresponds to the zone of crystallographic water.[58,59] The latter signals suggest that some of the excess of enriched water used in the syntheses was incorporated into the hydrated crystal structures. When focussing on the carbonate zone (**Figure 3A**, orange), the ^{17}O NMR spectra manifested under two forms: either as distorted gaussian lineshapes (*e.g.*, $Na_2CO_3{\cdot}H_2O$ and $K_2CO_3{\cdot}1.5H_2O$), or as broader asymmetric lineshapes (*e.g.*, $NaHCO_3$, $KHCO_3$, and Na_2CO_3) featuring a series of discontinuities (*i.e.*, steps, horns, shoulders, and/or feet) typical of second-order quadrupolar central transition (CT, –½ ↔ +½) patterns.[60] In particular, upon closer examination of the ^{17}O NMR spectra of the two bicarbonates, we noticed the presence of steps on the left. This is indicative of an overlap of several ^{17}O NMR signals, as expected from the reported crystal structures, as both $NaHCO_3$ and $KHCO_3$ have 3 crystallographically distinct oxygen environments (2 C=O and 1 C–OH, see supporting information). Yet, no distinct signature of the C–OH group of the bicarbonate ions was resolved directly from these 1D ^{17}O ssNMR spectra recorded at 14.1 T.

To achieve better resolution of the overlapping ^{17}O resonances in the bicarbonate/carbonate region, the ^{17}O MAS ssNMR spectra of Na_2CO_3, $K_2CO_3{\cdot}1.5H_2O$, $NaHCO_3$ and $KHCO_3$ (**Figure 3B**) were acquired at 28.2 T (1.2 GHz instrument) with sample temperatures of *ca*. 297 K. Certainly, a significant gain in resolution can be achieved for half-integer quadrupolar nuclei when working at higher fields, since the broadening caused by the second-order quadrupolar interaction scales inversely proportional with the magnetic field.[60] For Na_2CO_3 and $K_2CO_3{\cdot}1.5H_2O$, the general appearance of the ^{17}O NMR lineshapes at 28.2 T remain similar to the aforementioned 14.1 T ones, albeit much narrower. More importantly, for the bicarbonates, we can now clearly see the presence of two spectral regions (**Figure 3B**), which can be assigned to the oxygens belonging to the carbonyl (C=O) and hydroxyl (C–OH) oxygens of HCO_3^-. Complementary ^{1}H-^{17}O HMQC and INEPT NMR experiments were performed to confirm this attribution, as further discussed below (**Figure S12** and **S13**). At this stage, we note that the C–OH resonance was not observed in the recently reported natural-abundance ^{17}O NMR spectrum of $KHCO_3$, which may be due to the lack of sensitivity (non-labeled sample) and/or to the measurement conditions used (as further discussed in **Figure S14**).[19]

A first fit of the ^{17}O NMR spectra acquired at 28.2 T for the two bicarbonate salts is proposed in **Figure S15**. Three sites were used in the fits (2 C=O and 1 C–OH), in accordance

with the number of crystallographically distinct oxygen environments in the two structures. Regarding the C=O region (**Figure S15**, green and blue-shaded resonance**s)**, the assignments of the O1 and O2 resonances was made possible by using 1D and 2D ^{1}H-^{17}O HMQC/INEPT NMR experiments, allowing to distinguish which of the two signals is H-bonded to the C–OH (C=O···HO–C), and thus corresponds to O2 (**Figures S13** and **S14**). Overall, from our fits, the NMR parameters were then determined to be as follows, for $KHCO_3$ and $NaHCO_3$, respectively:
* O1 (C=O): δ_{iso} = 190.6 and 175.9 ppm, C_Q = 7.30 and 7.21 MHz, and η_Q = 0.73 and 0.83;
* O2 (C=O): δ_{iso} = 178.7 and 171.5 ppm, C_Q = 6.75 and 6.58 MHz, and η_Q = 0.64 and 1.00;
* O3 (C–OH): δ_{iso} = 146.9 and 137.7 ppm, C_Q = 7.30 and 7.65 MHz, and η_Q = 0.21 and 0.39.

Here, we note that an early ^{17}O nuclear quadrupole resonance (NQR) study of $NaHCO_3$ and $KHCO_3$ at 291 K had reported similar C_Q and η_Q values for O2 and O3, alongside the same assignment for these sites (see **Table S9**).[61] Yet, to the best of our knowledge, it is the first time that experimental values of δ_{iso} for C–OH groups in these bicarbonate salts are reported. Interestingly, the δ_{iso} values for C–OH and C=O groups were found to be higher for $KHCO_3$ than $NaHCO_3$. Such a trend had been observed in a computational study by Wong *et al.* on metal oxalates, where the ^{17}O isotropic chemical shifts were found to increase along the alkali-metal series with increasing ion size (*i.e.*, $Li^+ < Na^+ < K^+ < Rb^+ < Cs^+$).[57]

Taken together, these first ^{17}O NMR spectra of Na- and K- (bi)carbonate salts demonstrate several significant points. On one hand, the efficient ^{17}O-labeling using mechanochemistry enabled both improved sensitivity *and* spectral resolution. It allowed the acquisition of high-quality 1D ssNMR spectra in just a few scans, which is a major advantage compared to natural abundance studies,[19] as it provided direct evidence of the spectral signature of the C-OH group in the bicarbonates. Moreover, as shown for $KHCO_3$, further resolution could be readily achieved using 2D experiments: a ^{1}H-^{17}O HMQC spectrum was obtained in only 8 minutes at 28.2 T, from which the two inequivalent C=O sites could be assigned. On the other hand, the full spectral assignments of $KHCO_3$ and $NaHCO_3$ enabled to demonstrate that the range of variation of ^{17}O NMR parameters for (bi)carbonate anions extends beyond the recently reported values,[19] especially in the case of C–OH groups (**Figure S16** and **Table S9**), as further supported by DFT calculations (**Table S8**). Such features are highly promising for future studies on more complex (bi)carbonate containing materials by ^{17}O ssNMR.

Despite all the above advantages, only the spectra of the two bicarbonate salts were well resolved at 28.2 T, with the number of distinct ^{17}O NMR resonances in agreement with the crystal structures. In contrast, for $Na_2CO_3{\cdot}H_2O$ and $K_2CO_3{\cdot}1.5H_2O$, gaussian-like narrow

spectra were obtained, suggesting the presence of molecular-level motions around the anions (**Figure 3**). Indeed, dynamics can influence the local environments of oxygen, and, depending on their timescale, affect the ^{17}O ssNMR lineshapes (narrowing of the signal and loss in spectral features and resolution), as shown in several previous studies including on carbonates.[18,19,21] For the anhydrous Na_2CO_3 phase, we also observed a narrowing of the ^{17}O signal when heating the sample at only *ca.* 310 K.

To "freeze" these dynamics, and thereby try to recover the second-order ^{17}O quadrupolar lineshapes of all the distinct oxygen sites, ^{17}O MAS NMR spectra of the Na- and K- carbonate salts were recorded at ultra-low temperatures (*i.e.*, sample temperatures *ca*. 105 K). The data acquired at 14.1 T (600 MHz instrument) are shown in **Figure S17** (blue spectra). In these conditions, *all* spectra now appear as well-defined ^{17}O NMR second-order quadrupolar lineshapes. This is particularly noteworthy for $Na_2CO_3{\cdot}H_2O$ and $K_2CO_3{\cdot}1.5H_2O$, which did not show any such features at higher temperature (*ca.* 265 K). The complete analysis of these low-temperature spectra, including the extraction of the ^{17}O ssNMR parameters of each site and their interpretation based on the local structure around the oxygens, is currently under way, and will be reported in a forthcoming publication. Yet, at this stage, this result highlights that for materials developed for carbon-capture, ultra-low temperature ^{17}O ssNMR analyses can provide additional means for identifying the distinct (bi)carbonate local environments in presence. Moreover, it shows that a precise control of the actual sample temperature is needed, to enable robust comparisons of the (bi)carbonate local structure and motions between different samples. Based on these different observations, we then decided to study how ^{17}O ssNMR may unveil yet unexplored aspects of carbonate reactivity, in conditions closer to "real-life" application of carbon-capture materials.

2.3 Reactivity of Carbonates in the Presence of Water

In the development of novel materials for carbon capture, the study of the influence of water on the physi- and chemisorption of CO_2 has been shown to be critical. This holds true not only for purely inorganic sorbents like zeolites and layered double hydroxides (LDHs),[62,63] but also for porous hybrid materials like MOFs.[64,65] A wide variety of experimental and computational tools have thus been used to investigate the local structure and dynamics around H_2O and CO_2 (or (bi)carbonate ions), including using ^{17}O NMR.[19,25,66] Notably, two studies (one on LDH, the other on MOFs),[14,19,25] have shown ^{17}O isotope exchanges taking place between CO_2 (or

carbonates) and water, the latter being present within the interlayer spacings, pores, or at the surface of the material. Yet, despite the fact that such isotopic exchanges are widely studied in geology (essentially looking at the ^{18}O isotopes),[54–56] similar analyses are still rare in the study of carbon-capture materials, especially for ^{17}O. Here, given that the signatures of water and (bi)carbonates can be distinctly resolved by ^{17}O NMR, we decided to use the hydrated carbonates described above to probe isotopic exchange processes between water and (bi)carbonates, using *in-situ* analyses.

For these investigations, a ^{17}O-enriched $Na_2CO_3{\cdot}H_2O$ phase, with selective enrichment on the water, was synthesized using mechanochemistry (see **Supplementary Information S3** for details). The identity and purity of the sample were verified by pXRD and IR (**Figure 4A** and **4B**), and the lack of any substantial labeling of the carbonate was confirmed by the latter technique. *In-situ* variable temperature ^{17}O NMR experiments were thus recorded at 14.1 T (**Figure 4C**), in tandem with ^{1}H NMR analyses (**Figure S19**).

The first NMR experiments were carried out with the sample temperature regulated at 310 K. A broad ^{17}O NMR signal characteristic of crystalline H_2O was observed between 0 and –120 ppm. No signals were present in the spectral region between 200 and 40 ppm, confirming the absence of any significant (bi)carbonate labeling (**Figure 4C**, regions highlighted in blue and orange, respectively). ^{1}H NMR revealed the presence of a small amount of residual surface/mobile water in the sample (sharp ^{1}H resonance around 5.1 ppm), which had not been detected initially in ^{17}O NMR due to the analytical conditions used (**Figure S18**).

Following this, the sample temperature was increased in increments of 20 K, with spectra recorded at each step under identical conditions, up to a maximum sample temperature of 370 K. Shown in **Figure 4** are a sub-set of these spectra, with the full range of ^{17}O experiments and accompanying ^{1}H data in **Figures S18** and **S19**. The ^{17}O NMR spectrum recorded at 370 K was found to be nearly identical to the one initially recorded at 310 K. However, when the sample was then cooled to 290 K, we observed the appearance of a second signal centered around 119 ppm (*i.e.*, in the region characteristic of (bi)carbonates). More specifically, this signal was found precisely at the resonance of the carbonate ions in $Na_2CO_3{\cdot}H_2O$ at ambient temperature (**Figure S20**). When the sample was then reheated to 370 K, the disappearance of the carbonate peak was observed, and the only signal visible was that of crystalline H_2O. Following these *in-situ* NMR analyses, the rotor was weighed, showing that no weight loss had occurred during the measurements. Additionally, the sample was characterized once more by pXRD and IR spectroscopy, revealing no noticeable change in phase (**Figure 4A** and **4B**).

Overall, these *in-situ* NMR analyses demonstrate that *(i)* isotopic exchange between the enriched water and the initially non-labeled carbonates of $Na_2CO_3{\cdot}H_2O$ can occur at 370 K, and *(ii)* carbonate ions which undergo a fast ^{17}O-isotopic exchange with water may not be observable in ^{17}O MAS NMR spectra under certain measurement and/or sample preparation conditions (as shown here at 370 K), despite their presence in the sample.

Several explanations can be proposed to the carbonate labeling observed during the *in-situ* VT ^{17}O NMR experiments. First, the small excess of surface/absorbed water may enable the dissolution of part of the $Na_2CO_3{\cdot}H_2O$ phase, thereby allowing an isotopic exchange process in "solution", involving the transient formation of hydrated CO_2, as proposed in the mechanism similar of carbonate enrichment in ^{18}O-labeled water.[54–56] Second, the *in-situ* NMR measurement conditions (temperature and MAS-induced pressure) may enable the transient formation of another type of intermediate between the crystalline H_2O and CO_3^{2-} (*e.g.*, an orthocarbonate-like species), which could allow for the intermolecular isotopic exchange to occur in the crystalline phase.[d] In both cases, we note that we did not observe ^{17}O NMR signals of carbonate-related ions (*ca.* 200 to 180 ppm) nor $CO_{2\,(aq)}$ (*ca.* 80 to 60 ppm) in any of the spectra, even when performing the analyses using the simple Bloch-decay NMR sequence. Further analyses would be needed to pinpoint how and at what rate the isotopic exchange occurs at the molecular scale, which is beyond the scope of the present work.

Albeit preliminary, the *in-situ* ^{17}O NMR analyses shown above have several implications. First, thanks to a selective labeling of the monohydrate, they could be used to reveal the existence of oxygen-isotopic exchange processes, which could become a new handle to study and compare different materials developed for carbon capture. Second, from a more practical perspective, they show that precaution should be taken in the interpretation of the ^{17}O MAS NMR spectra recorded for carbonate-containing phases in presence of water, because resonances relative to enriched (bi)carbonate ions may not be visible due to fast chemical exchanges with neighbouring water (as here for the 370 K data). Based on this observation, we would recommend performing analyses at two different temperatures at least (bearing in mind that equilibria can be shifted upon changes in temperature), to avoid missing out on chemical information. Lastly, beyond the study of materials for carbon capture applications, the observation of partial ^{17}O-isotopic labeling of the carbonates of $Na_2CO_3.H_2{*}O$ at high

[d] Generally the formation of orthocarbonates requires high pressures, and we have no experimental evidence of their presence in our conditions. These species are simply mentioned here, because their transient formation could be a way of explaining the isotope exchanges.

temperature suggests that it may be possible to directly label hydrated carbonate salts using a "liquid-assisted grinding" approach, while including heating during the milling. With the increasing number of heating set-ups being developed for ball-milling equipment,[67,68] the latter option appears as very valuable to help further expand the scope of carbonate-labeled precursors for other ^{17}O NMR applications, which we are continuing to investigate with on-going work in our lab.

3. Conclusion

In this manuscript, we have described a new strategy for the ^{17}O-enrichment of Na- and K- (bi)carbonate salts, using mechanochemistry. The synthetic approach is robust, user-friendly, and cost-effective, enabling the production of up to 400 mg of labeled Na_2CO_3 in just half a day of manipulation. The high enrichment levels achieved enabled the first high resolution ^{17}O solid-state NMR analyses to be performed on these materials in short experimental times (as short as 8 minutes for some of the 2D measurements). This enabled carrying out the studies at not only different magnetic fields, but also different temperatures, thereby shedding light on important features regarding the ^{17}O NMR signatures of (bi)carbonates in solids, among which (*i*) broad ranges in the variation of the ^{17}O NMR parameters of C=O and C–OH groups of (bi)carbonates, with notably distinct signatures for the hydroxyl group in $NaHCO_3$ and $KHCO_3$; (*ii*) a strong sensitivity of their ^{17}O NMR parameters to temperature (with direct impact on the quadrupolar lineshapes), especially for the hydrated phases, which appeared as "gaussian-like" resonances on the spectra recorded at *ca*. 265 K.

The high ^{17}O-isotopic labeling achieved on the (bi)carbonate phases was shown to be critical not just to enable accurate spectral fitting, but also to avoid missing out on some resonances at natural abundance (which can lead to erroneous interpretations of the spectra), and to help elucidate under-studied aspects of the reactivity of (bi)carbonate ions in solids, namely oxygen isotope-transfer processes. From this work, it appears that any future ^{17}O NMR study of materials developed for carbon-capture applications will require an accurate control of the temperature, and also analyses at different temperatures, in order to avoid missing out on resonances, leading to mis-interpretations (or over interpretations) of the data. As such, the present work provides sound bases for future works on (bi)carbonate-based materials (including those developed for CO_2 capture), for which structure, reactivity, and speciation aspects are key.

Beyond the aforementioned applications, the possibility of labeling with ^{17}O Na- and K-(bi)carbonate salts opens new avenues to the study of a plethora of systems by ^{17}O MAS NMR, as these compounds are widely used as precursors for the synthesis of functional (bio)materials. Moreover, the labeling procedure proposed herein (involving CDI) is *a priori* applicable to the enrichment of other metal carbonates (including with transition-metal and lanthanide ions), which could then be engaged for the preparation of functional ceramics and glasses, for which ^{17}O ssNMR is invaluable for establishing structure/property correlations. Last but not least, Na- and K- (bi)carbonates decompose thermally by release of CO_2, with a temperature as low as 80 °C for $NaHCO_3$. These reagents could therefore be used as simple and straightforward source for production of enriched CO_2. The latter could then be used for studying materials for carbon capture using high resolution ^{17}O NMR (which is at the moment, largely inaccessible, due to difficulties in purchasing enriched CO_2 gas, *vide supra*). Moreover, the labeled CO_2 produced upon decomposition of (bi)carbonates, could also be used for synthesizing other ^{17}O-labeled molecules,[69] thereby contributing to the study of their structure and reactivity. These are points we endeavour to look into, with on-going efforts in our research group.

Data Availability

Complementary IR, pXRD, MS, and NMR analyses including NMR acquisition parameters supporting this article have been uploaded as part of the electronic supporting information (ESI).† All data can be made available upon reasonable demand.

Author Contributions

AP, NF and DL conducted the majority of the research experiments (syntheses, general characterizations and ssNMR analyses). CE contributed to the early stages of the project, by performing the initial syntheses. TXM contributed to the discussion on the mechanochemical syntheses. AP performed the GIPAW-DFT calculations, in close collaboration with CG. CG participated in all discussions regarding computational results. FMV and FS carried out the low-temperature ^{17}O ssNMR studies at 14.1 T, and DG participated to those at 18.8 T. JT assisted in the ultra-high field ssNMR analyses at 28.2 T. FV an NP performed the MS analyses

on the ^{18}O-labeled compounds. AP and DL wrote the first draft of the manuscript, and all authors contributed to the final preparation of the manuscript.

Conflicts of Interest

There are no conflicts of interest to declare.

Acknowledgements

This project is funded in part by the European Research Council (ERC) under the European Union's Horizon 2020 research and innovation program (grant agreement no. 772204; 2017 ERC COG, MISOTOP project. Further financial support from the INFRANALYTICS FR2054 for conducting NMR experiments at the CRMN in Lyon and USSC in Lille. NMR research was also conducted at the National High Magnetic Field Laboratory (NHMFL, Tallahassee) in Florida, which is supported by the National Science Foundation Cooperative Agreements (No. DMR-2128556), the State of Florida and a partial support by National Institutes of Health Grant RM1-GM148766. This project has received support from the European Union's Horizon 2020 research and innovation programme under Grant Agreement 101008500 (PANACEA) and F.J.S is supported by the postdoctoral scholar award from the Provost's Office at Florida State University. DFT computations were run using high performance computing resources from GENCI-IDRIS (grants no. 2024-AD010815148 and AD10-097535). Philippe Gaveau (ICG, Montpellier) and Andrew Rankin (USSC, Lille) are thanked for their experimental expertise and assistance on part of the ssNMR analyses. Dr Jessica Novák-Špačková is warmly acknowledged for early discussions related to this work, Dr Hugo Petitjean for exchanges about the IR data, and Dr Ieva Goldberga for assistance in some initial experiments.

References

(1) Calvin, K.; Dasgupta, D.; Krinner, G.; Mukherji, A.; Thorne, P. W.; Trisos, C.; Romero, J.; Aldunce, P.; Barrett, K.; Blanco, G.; Cheung, W. W. L.; Connors, S.; Denton, F.; Diongue-Niang, A.; Dodman, D.; Garschagen, M.; Geden, O.; Hayward, B.; Jones, C.; Jotzo, F.; Krug, T.; Lasco, R.; Lee, Y.-Y.; Masson-Delmotte, V.; Meinshausen, M.; Mintenbeck, K.; Mokssit, A.; Otto, F. E. L.; Pathak, M.; Pirani, A.; Poloczanska, E.; Pörtner, H.-O.; Revi, A.; Roberts, D. C.; Roy, J.; Ruane, A. C.; Skea, J.; Shukla, P. R.; Slade, R.; Slangen, A.; Sokona, Y.; Sörensson, A. A.; Tignor, M.; van Vuuren, D.; Wei, Y.-M.; Winkler, H.; Zhai, P.; Zommers, Z.; Hourcade, J.-C.; Johnson, F. X.; Pachauri, S.; Simpson, N. P.; Singh, C.; Thomas, A.; Totin, E.; Alegría, A.; Armour, K.; Bednar-Friedl, B.; Blok, K.; Cissé, G.; Dentener, F.; Eriksen, S.; Fischer, E.; Garner, G.; Guivarch, C.; Haasnoot, M.; Hansen, G.; Hauser, M.; Hawkins, E.; Hermans, T.; Kopp, R.; Leprince-Ringuet, N.; Lewis, J.; Ley, D.; Ludden, C.; Niamir, L.; Nicholls, Z.; Some, S.; Szopa, S.; Trewin, B.; van der Wijst, K.-I.; Winter, G.; Witting, M.; Birt, A.; Ha, M. *IPCC, 2023: Climate Change 2023: Synthesis Report. Contribution of Working Groups I, II and III to the Sixth Assessment Report of the Intergovernmental Panel on Climate Change [Core Writing Team, H. Lee and J. Romero (Eds.)]. IPCC, Geneva, Switzerland.*; 2023. https://www.ipcc.ch/report/ar6/syr/.

(2) Matthews, H. D.; Wynes, S. Current Global Efforts Are Insufficient to Limit Warming to 1.5°C. *Science.* **2022**, *376* (6600), 1404–1409. https://doi.org/10.1126/science.abo3378.

(3) Snæbjörnsdóttir, S. Ó.; Sigfússon, B.; Marieni, C.; Goldberg, D.; Gislason, S. R.; Oelkers, E. H. Carbon Dioxide Storage through Mineral Carbonation. *Nat. Rev. Earth Environ.* **2020**, *1* (2), 90–102. https://doi.org/10.1038/s43017-019-0011-8.

(4) ten Have, I. C.; van den Brink, R. Y.; Marie-Rose, S. C.; Meirer, F.; Weckhuysen, B. M. Using Biomass Gasification Mineral Residue as Catalyst to Produce Light Olefins from CO, CO_2, and H_2 Mixtures. *ChemSusChem* **2022**, *15* (11). https://doi.org/10.1002/cssc.202200436.

(5) Hamdy, L. B.; Goel, C.; Rudd, J. A.; Barron, A. R.; Andreoli, E. The Application of Amine-Based Materials for Carbon Capture and Utilisation: An Overarching View. *Mater. Adv.* **2021**, *2* (18), 5843–5880. https://doi.org/10.1039/D1MA00360G.

(6) Lackner, K. S.; Wendt, C. H.; Butt, D. P.; Joyce, E. L.; Sharp, D. H. Carbon Dioxide Disposal in Carbonate Minerals. *Energy* **1995**, *20* (11), 1153–1170.

https://doi.org/10.1016/0360-5442(95)00071-N.

(7) Santos, H. S.; Nguyen, H.; Venâncio, F.; Ramteke, D.; Zevenhoven, R.; Kinnunen, P. Mechanisms of Mg Carbonates Precipitation and Implications for CO_2 Capture and Utilization/Storage. *Inorg. Chem. Front.* **2023**, *10* (9), 2507–2546. https://doi.org/10.1039/D2QI02482A.

(8) Hills, T. P.; Sceats, M.; Rennie, D.; Fennell, P. LEILAC: Low Cost CO_2 Capture for the Cement and Lime Industries. *Energy Procedia* **2017**, *114* (November 2016), 6166–6170. https://doi.org/10.1016/j.egypro.2017.03.1753.

(9) Zick, M. E.; Cho, D.; Ling, J.; Milner, P. J. Carbon Capture Beyond Amines: CO_2 Sorption at Nucleophilic Oxygen Sites in Materials. *ChemNanoMat* **2023**, *9* (1). https://doi.org/10.1002/cnma.202200436.

(10) Li, Z.; Liu, P.; Ou, C.; Dong, X. Porous Metal–Organic Frameworks for Carbon Dioxide Adsorption and Separation at Low Pressure. *ACS Sustain. Chem. Eng.* **2020**, *8* (41), 15378–15404. https://doi.org/10.1021/acssuschemeng.0c05155.

(11) Ding, M.; Flaig, R. W.; Jiang, H.-L.; Yaghi, O. M. Carbon Capture and Conversion Using Metal–Organic Frameworks and MOF-Based Materials. *Chem. Soc. Rev.* **2019**, *48* (10), 2783–2828. https://doi.org/10.1039/C8CS00829A.

(12) Vismara, R.; Terruzzi, S.; Maspero, A.; Grell, T.; Bossola, F.; Sironi, A.; Galli, S.; Navarro, J. A. R.; Colombo, V. CO_2 Adsorption in a Robust Iron(III) Pyrazolate-Based MOF: Molecular-Level Details and Frameworks Dynamics From Powder X-ray Diffraction Adsorption Isotherms. *Adv. Mater.* **2024**, *36* (12). https://doi.org/10.1002/adma.202209907.

(13) Pugh, S. M.; Forse, A. C. Nuclear Magnetic Resonance Studies of Carbon Dioxide Capture. *J. Magn. Reson.* **2023**, *346*, 107343. https://doi.org/10.1016/j.jmr.2022.107343.

(14) Berge, A. H.; Pugh, S. M.; Short, M. I. M. M.; Kaur, C.; Lu, Z.; Lee, J.-H.; Pickard, C. J.; Sayari, A.; Forse, A. C. Revealing Carbon Capture Chemistry with 17-Oxygen NMR Spectroscopy. *Nat. Commun.* **2022**, *13* (1), 7763. https://doi.org/10.1038/s41467-022-35254-w.

(15) Pereira, D.; Fonseca, R.; Marin-Montesinos, I.; Sardo, M.; Mafra, L. Understanding CO_2 Adsorption Mechanisms in Porous Adsorbents: A Solid-State NMR Survey. *Curr. Opin. Colloid Interface Sci.* **2023**, *64*, 101690. https://doi.org/10.1016/j.cocis.2023.101690.

(16) Wu, G. Alkali Metal NMR of Biological Molecules. In *Encyclopedia of Magnetic Resonance*; John Wiley & Sons, Ltd: Chichester, UK, 2011; Vol. 2011. https://doi.org/10.1002/9780470034590.emrstm1210.

(17) Kong, X.; O'Dell, L. A.; Terskikh, V.; Ye, E.; Wang, R.; Wu, G. Variable-Temperature ^{17}O NMR Studies Allow Quantitative Evaluation of Molecular Dynamics in Organic Solids. *J. Am. Chem. Soc.* **2012**, *134* (35), 14609–14617. https://doi.org/10.1021/ja306227p.

(18) Dunstan, M. T.; Griffin, J. M.; Blanc, F.; Leskes, M.; Grey, C. P. Ion Dynamics in Li_2CO_3 Studied by Solid-State NMR and First-Principles Calculations. *J. Phys. Chem. C* **2015**, *119* (43), 24255–24264. https://doi.org/10.1021/acs.jpcc.5b06647.

(19) Rhodes, B. J.; Schaaf, L. L.; Zick, M. E.; Pugh, S. M.; Jordon, S.; Sharma, S.; Wade, C. R.; Milner, P. J.; Forse, A. C. ^{17}O NMR Spectroscopy Reveals CO_2 Speciation and Dynamics in Hydroxide-Based Carbon Capture Materials . **2024**. https://doi.org/10.26434/chemrxiv-2024-c0vmg.

(20) Beerwerth, J.; Siegel, R.; Hoffmann, L.; Plaga, L. S.; Storek, M.; Bojer, B.; Senker, J.; Hiller, W.; Böhmer, R. From Ultraslow to Extremely Fast Dynamics in Sodium Nitrate: An ^{17}O NMR Study. *Appl. Magn. Reson.* **2020**, *51* (7), 597–620. https://doi.org/10.1007/s00723-020-01201-5.

(21) Nava, M.; Lopez, N.; Müller, P.; Wu, G.; Nocera, D. G.; Cummins, C. C. Anion-Receptor Mediated Oxidation of Carbon Monoxide to Carbonate by Peroxide Dianion. *J. Am. Chem. Soc.* **2015**, *137* (46), 14562–14565. https://doi.org/10.1021/jacs.5b08495.

(22) Wang, W. D.; Lucier, B. E. G.; Terskikh, V. V.; Wang, W.; Huang, Y. Wobbling and Hopping: Studying Dynamics of CO_2 Adsorbed in Metal–Organic Frameworks via ^{17}O Solid-State NMR. *J. Phys. Chem. Lett.* **2014**, *5* (19), 3360–3365. https://doi.org/10.1021/jz501729d.

(23) Hu, M. Y.; Deng, X.; Thanthiriwatte, K. S.; Jackson, V. E.; Wan, C.; Qafoku, O.; Dixon, D. A.; Felmy, A. R.; Rosso, K. M.; Hu, J. Z. In Situ Natural Abundance ^{17}O and ^{25}Mg NMR Investigation of Aqueous $Mg(OH)_2$ Dissolution in the Presence of Supercritical CO 2. *Environ. Sci. Technol.* **2016**, *50* (22), 12373–12384. https://doi.org/10.1021/acs.est.6b03443.

(24) Du, J.-H.; Chen, L.; Zhang, B.; Chen, K.; Wang, M.; Wang, Y.; Hung, I.; Gan, Z.; Wu, X.-P.; Gong, X.-Q.; Peng, L. Identification of CO_2 Adsorption Sites on MgO Nanosheets by Solid-State Nuclear Magnetic Resonance Spectroscopy. *Nat. Commun.* **2022**, *13* (1), 707. https://doi.org/10.1038/s41467-022-28405-6.

(25) Sahoo, P.; Ishihara, S.; Yamada, K.; Deguchi, K.; Ohki, S.; Tansho, M.; Shimizu, T.; Eisaku, N.; Sasai, R.; Labuta, J.; Ishikawa, D.; Hill, J. P.; Ariga, K.; Bastakoti, B. P.; Yamauchi, Y.; Iyi, N. Rapid Exchange between Atmospheric CO_2 and Carbonate Anion

Intercalated within Magnesium Rich Layered Double Hydroxide. *ACS Appl. Mater. Interfaces* **2014**, *6* (20), 18352–18359. https://doi.org/10.1021/am5060405.

(26) Metz, G.; Wu, X. L.; Smith, S. O. Ramped-Amplitude Cross Polarization in Magic-Angle-Spinning NMR. *J. Magn. Reson. Ser. A* **1994**, *110* (2), 219–227. https://doi.org/10.1006/jmra.1994.1208.

(27) Comellas, G.; Lopez, J. J.; Nieuwkoop, A. J.; Lemkau, L. R.; Rienstra, C. M. Straightforward, Effective Calibration of SPINAL-64 Decoupling Results in the Enhancement of Sensitivity and Resolution of Biomolecular Solid-State NMR. *J. Magn. Reson.* **2011**, *209* (2), 131–135. https://doi.org/10.1016/j.jmr.2010.12.011.

(28) Fung, B. M.; Khitrin, A. K.; Ermolaev, K. An Improved Broadband Decoupling Sequence for Liquid Crystals and Solids. *J. Magn. Reson.* **2000**, *142* (1), 97–101. https://doi.org/10.1006/jmre.1999.1896.

(29) Iuga, D.; Schäfer, H.; Verhagen, R.; Kentgens, A. P. . Population and Coherence Transfer Induced by Double Frequency Sweeps in Half-Integer Quadrupolar Spin Systems. *J. Magn. Reson.* **2000**, *147* (2), 192–209. https://doi.org/10.1006/jmre.2000.2192.

(30) Gómez, J. S.; Rankin, A. G. M.; Trébosc, J.; Pourpoint, F.; Tsutsumi, Y.; Nagashima, H.; Lafon, O.; Amoureux, J.-P. Improved NMR Transfer of Magnetization from Protons to Half-Integer Spin Quadrupolar Nuclei at Moderate and High Magic-Angle Spinning Frequencies. *Magn. Reson.* **2021**, *2* (1), 447–464. https://doi.org/10.5194/mr-2-447-2021.

(31) Harris, R. K.; Becker, E. D.; Cabral de Menezes, S. M.; Granger, P.; Hoffman, R. E.; Zilm, K. W. Further Conventions for NMR Shielding and Chemical Shifts (IUPAC Recommendations 2008). *Pure Appl. Chem.* **2008**, *80* (1), 59–84. https://doi.org/10.1351/pac200880010059.

(32) van Meerten, S. G. J.; Franssen, W. M. J.; Kentgens, A. P. M. SsNake: A Cross-Platform Open-Source NMR Data Processing and Fitting Application. *J. Magn. Reson.* **2019**, *301*, 56–66. https://doi.org/10.1016/j.jmr.2019.02.006.

(33) Thurber, K. R.; Tycko, R. Measurement of Sample Temperatures under Magic-Angle Spinning from the Chemical Shift and Spin-Lattice Relaxation Rate of ^{79}Br in KBr Powder. *J. Magn. Reson.* **2009**, *196* (1), 84–87. https://doi.org/10.1016/j.jmr.2008.09.019.

(34) Arakcheeva, A.; Bindi, L.; Pattison, P.; Meisser, N.; Chapuis, G.; Pekov, I. The Incommensurately Modulated Structures of Natural Natrite at 120 and 293 K from Synchrotron X-Ray Data. *Am. Mineral.* **2010**, *95* (4), 574–581.

https://doi.org/10.2138/am.2010.3384.

(35) Sharma, B. D. Sodium Bicarbonate and Its Hydrogen Atom. *Acta Crystallogr.* **1965**, *18* (4), 818–819. https://doi.org/10.1107/S0365110X65001895.

(36) Wu, K. K.; Brown, I. D. A Neutron Diffraction Study of $Na_2CO_3.H_2O$. *Acta Crystallogr. Sect. B Struct. Crystallogr. Cryst. Chem.* **1975**, *31* (3), 890–892. https://doi.org/10.1107/S0567740875004001.

(37) Skakle, J. M. S.; Wilson, M.; Feldmann, J. Dipotassium Carbonate Sesquihydrate: Rerefinement against New Intensity Data. *Acta Crystallogr. Sect. E Struct. Reports Online* **2001**, *57* (11), i94–i97. https://doi.org/10.1107/S1600536801016312.

(38) Becht, H. Y.; Struikmans, R. A Monoclinic High-Temperature Modification of Potassium Carbonate. *Acta Crystallogr. Sect. B Struct. Crystallogr. Cryst. Chem.* **1976**, *32* (12), 3344–3346. https://doi.org/10.1107/S0567740876010303.

(39) Kresse, G.; Furthmüller, J. Efficiency of Ab-Initio Total Energy Calculations for Metals and Semiconductors Using a Plane-Wave Basis Set. *Comput. Mater. Sci.* **1996**, *6* (1), 15–50. https://doi.org/10.1016/0927-0256(96)00008-0.

(40) Kresse, G.; Furthmüller, J. Efficient Iterative Schemes for *Ab Initio* Total-Energy Calculations Using a Plane-Wave Basis Set. *Phys. Rev. B* **1996**, *54* (16), 11169–11186. https://doi.org/10.1103/PhysRevB.54.11169.

(41) Kresse, G.; Hafner, J. Ab Initio Molecular Dynamics for Liquid Metals. *Phys. Rev. B* **1993**, *47* (1), 558–561. https://doi.org/10.1103/PhysRevB.47.558.

(42) Hammer, B.; Hansen, L. B.; Nørskov, J. K. Improved Adsorption Energetics within Density-Functional Theory Using Revised Perdew-Burke-Ernzerhof Functionals. *Phys. Rev. B* **1999**, *59* (11), 7413–7421. https://doi.org/10.1103/PhysRevB.59.7413.

(43) Grimme, S.; Antony, J.; Ehrlich, S.; Krieg, H. A Consistent and Accurate *Ab Initio* Parametrization of Density Functional Dispersion Correction (DFT-D) for the 94 Elements H-Pu. *J. Chem. Phys.* **2010**, *132* (15), 154104. https://doi.org/10.1063/1.3382344.

(44) Giannozzi, P.; Baroni, S.; Bonini, N.; Calandra, M.; Car, R.; Cavazzoni, C.; Ceresoli, D.; Chiarotti, G. L.; Cococcioni, M.; Dabo, I.; Dal Corso, A.; de Gironcoli, S.; Fabris, S.; Fratesi, G.; Gebauer, R.; Gerstmann, U.; Gougoussis, C.; Kokalj, A.; Lazzeri, M.; Martin-Samos, L.; Marzari, N.; Mauri, F.; Mazzarello, R.; Paolini, S.; Pasquarello, A.; Paulatto, L.; Sbraccia, C.; Scandolo, S.; Sclauzero, G.; Seitsonen, A. P.; Smogunov, A.; Umari, P.; Wentzcovitch, R. M. QUANTUM ESPRESSO: A Modular and Open-Source Software Project for Quantum Simulations of Materials. *J. Phys. Condens. Matter* **2009**,

21 (39), 395502. https://doi.org/10.1088/0953-8984/21/39/395502.

(45) Pickard, C. J.; Mauri, F. All-Electron Magnetic Response with Pseudopotentials: NMR Chemical Shifts. *Phys. Rev. B* **2001**, *63* (24), 245101. https://doi.org/10.1103/PhysRevB.63.245101.

(46) Perdew, J. P.; Burke, K.; Ernzerhof, M. Generalized Gradient Approximation Made Simple. *Phys. Rev. Lett.* **1996**, *77* (18), 3865–3868. https://doi.org/10.1103/PhysRevLett.77.3865.

(47) Kleinman, L.; Bylander, D. M. Efficacious Form for Model Pseudopotentials. *Phys. Rev. Lett.* **1982**, *48* (20), 1425–1428. https://doi.org/10.1103/PhysRevLett.48.1425.

(48) Pyykkö, P. Year-2017 Nuclear Quadrupole Moments. *Mol. Phys.* **2018**, *116* (10), 1328–1338. https://doi.org/10.1080/00268976.2018.1426131.

(49) Goldberga, I.; Hung, I.; Sarou-Kanian, V.; Gervais, C.; Gan, Z.; Novák-Špačková, J.; Métro, T. X.; Leroy, C.; Berthomieu, D.; van der Lee, A.; Bonhomme, C.; Laurencin, D. High-Resolution ^{17}O Solid-State NMR as a Unique Probe for Investigating Oxalate Binding Modes in Materials: The Case Study of Calcium Oxalate Biominerals. *Inorg. Chem.* **2024**, *63* (22), 10179–10193. https://doi.org/10.1021/acs.inorgchem.4c00300.

(50) Smith, M. E.; Steuernagel, S.; Whitfield, H. J. ^{17}O Magic-Angle Spinning Nuclear Magnetic Resonance of $CaCO_3$. *Solid State Nucl. Magn. Reson.* **1995**, *4* (5), 313–316. https://doi.org/10.1016/0926-2040(95)00010-N.

(51) Ihli, J.; Clark, J. N.; Kanwal, N.; Kim, Y.; Holden, M. A.; Harder, R. J.; Tang, C. C.; Ashbrook, S. E.; Robinson, I. K.; Meldrum, F. C. Visualization of the Effect of Additives on the Nanostructures of Individual Bio-Inspired Calcite Crystals. *Chem. Sci.* **2019**, *10* (4), 1176–1185. https://doi.org/10.1039/C8SC03733G.

(52) Leskes, M.; Moore, A. J.; Goward, G. R.; Grey, C. P. Monitoring the Electrochemical Processes in the Lithium–Air Battery by Solid State NMR Spectroscopy. *J. Phys. Chem. C* **2013**, *117* (51), 26929–26939. https://doi.org/10.1021/jp410429k.

(53) Rudolph, W. W.; Irmer, G.; Königsberger, E. Speciation Studies in Aqueous HCO_3^- – CO_3^{2-} Solutions. A Combined Raman Spectroscopic and Thermodynamic Study. *Dalt. Trans.* **2008**, No. 7, 900–908. https://doi.org/10.1039/B713254A.

(54) Geisler, T.; Perdikouri, C.; Kasioptas, A.; Dietzel, M. Real-Time Monitoring of the Overall Exchange of Oxygen Isotopes between Aqueous CO_3^{2-} and H_2O by Raman Spectroscopy. *Geochim. Cosmochim. Acta* **2012**, *90*, 1–11. https://doi.org/10.1016/j.gca.2012.04.058.

(55) Landuyt, A.; Kumar, P. V.; Yuwono, J. A.; Bork, A. H.; Donat, F.; Abdala, P. M.; Müller,

C. R. Uncovering the CO_2 Capture Mechanism of $NaNO_3$ -Promoted MgO by ^{18}O Isotope Labeling. *JACS Au* **2022**, *2* (12), 2731–2741. https://doi.org/10.1021/jacsau.2c00461.

(56) Wang, S.; Lu, K.; Wang, T.; Wu, J.; Zheng, H.; Huang, Y. A Method for Isotope Exchange Kinetics in Mineral-Water System–an in-Situ Study on Oxygen Isotope Exchange in Na_2CO_3-H_2O System. *Spectrochim. Acta Part A Mol. Biomol. Spectrosc.* **2020**, *241*, 118648. https://doi.org/10.1016/j.saa.2020.118648.

(57) Wong, A.; Thurgood, G.; Dupree, R.; Smith, M. E. A First-Principles Computational ^{17}O NMR Investigation of Metal Ion–Oxygen Interactions in Carboxylate Oxygens of Alkali Oxalates. *Chem. Phys.* **2007**, *337* (1–3), 144–150. https://doi.org/10.1016/j.chemphys.2007.07.007.

(58) Nour, S.; Widdifield, C. M.; Kobera, L.; Burgess, K. M. N.; Errulat, D.; Terskikh, V. V.; Bryce, D. L. Oxygen-17 NMR Spectroscopy of Water Molecules in Solid Hydrates. *Can. J. Chem.* **2016**, *94* (3), 189–197. https://doi.org/10.1139/cjc-2015-0547.

(59) Goldberga, I.; Patris, N.; Chen, C.-H.; Thomassot, E.; Trébosc, J.; Hung, I.; Gan, Z.; Berthomieu, D.; Métro, T.-X.; Bonhomme, C.; Gervais, C.; Laurencin, D. First Direct Insight into the Local Environment and Dynamics of Water Molecules in the Whewellite Mineral Phase: Mechanochemical Isotopic Enrichment and High-Resolution ^{17}O and ^{2}H NMR Analyses. *J. Phys. Chem. C* **2022**, *126* (29), 12044–12059. https://doi.org/10.1021/acs.jpcc.2c02070.

(60) Wasylishen, R. E.; Ashbrook, S. E.; Wimperis, S. NMR of Quadrupolar Nuclei in Solid Materials; John Wiley & Sons Ltd, 2012.

(61) Poplett, I. J. F.; Smith, J. A. S. Double Resonance Detection of ^{17}O Quadrupole Resonance in Potassium Bicarbonate. *J. Chem. Soc. Faraday Trans. 2* **1981**, *77* (5), 761. https://doi.org/10.1039/f29817700761.

(62) Boer, D. G.; Langerak, J.; Pescarmona, P. P. Zeolites as Selective Adsorbents for CO_2 Separation. *ACS Appl. Energy Mater.* **2023**, *6* (5), 2634–2656. https://doi.org/10.1021/acsaem.2c03605.

(63) Santamaría, L.; Korili, S. A.; Gil, A. Layered Double Hydroxides for CO_2 Adsorption at Moderate Temperatures: Synthesis and Amelioration Strategies. *Chem. Eng. J.* **2023**, *455* (November 2022), 140551. https://doi.org/10.1016/j.cej.2022.140551.

(64) Erucar, I.; Keskin, S. Unlocking the Effect of H_2O on CO_2 Separation Performance of Promising MOFs Using Atomically Detailed Simulations. *Ind. Eng. Chem. Res.* **2020**, *59* (7), 3141–3152. https://doi.org/10.1021/acs.iecr.9b05487.

(65) Rajendran, A.; Shimizu, G. K. H.; Woo, T. K. The Challenge of Water Competition in Physical Adsorption of CO_2 by Porous Solids for Carbon Capture Applications – A Short Perspective. *Adv. Mater.* **2024**, *36* (12). https://doi.org/10.1002/adma.202301730.

(66) Zhao, L.; Qi, Z.; Blanc, F.; Yu, G.; Wang, M.; Xue, N.; Ke, X.; Guo, X.; Ding, W.; Grey, C. P.; Peng, L. Investigating Local Structure in Layered Double Hydroxides with ^{17}O NMR Spectroscopy. *Adv. Funct. Mater.* **2014**, *24* (12), 1696–1702. https://doi.org/10.1002/adfm.201301157.

(67) Félix, G.; Fabregue, N.; Leroy, C.; Métro, T. X.; Chen, C. H.; Laurencin, D. Induction-Heated Ball-Milling: A Promising Asset for Mechanochemical Reactions. *Phys. Chem. Chem. Phys.* **2023**, *25* (35), 23435–23447. https://doi.org/10.1039/d3cp02540c. (and references therein).

(68) Cindro, N.; Tireli, M.; Karadeniz, B.; Mrla, T.; Užarević, K. Investigations of Thermally Controlled Mechanochemical Milling Reactions, *ACS Sustainable Chem. Eng.* **2019**, *7* (19), 16301–16309. https://doi.org/10.1021/acssuschemeng.9b03319.

(69) Porcheddu, A.; Maggi, R.; Cauzzi, A.; Maestri, G. $NaHCO_3$ as CO_2 solid surrogate for carboxylation reactions under mechaochemical conditions *ChemRxiv* **2024**. https://doi.org/10.26434/chemrxiv-2024-zm9fw ORCID:

Table 1: Examples of synthesis quantities used in the mechanochemical enrichment of sodium and potassium (bi)carbonate salts.

Product	Water	Mass of Hydroxide (mg)	Mass of CDI (mg)	Volume of Water (μL)	Product mass (mg)	Synthetic Yield (%)
$NaHCO_3$	^{16}O	45.6 [a]	368.0	80	76	92
	^{17}O	46.2 [a]	376.0	80	75	78
	^{18}O	46.4 [a]	376.9	80	80	82
$Na_2CO_3•H_2O$	^{16}O	140.7 [a]	219.3	48	117	82
	^{17}O	140.7 [a]	219.5	48	130	87
	^{18}O	140.7 [a]	219.3	48	125	91
$KHCO_3$	^{16}O	96.7 [b]	564.8	125	104	60
	^{17}O	93.8 [b]	541.7	120	119	71
	^{18}O	96.7 [b]	561.8	125	123	71
$K_2CO_3•1.5H_2O$	^{16}O	103.7 [b]	148.8	35	71	68
	^{17}O	110.1 [b]	160.1	35	93	57
	^{18}O	93.3 [b]	135.6	30	78	57

Hydroxides used as educts for synthesis: [a] NaOH and [b] KOH.

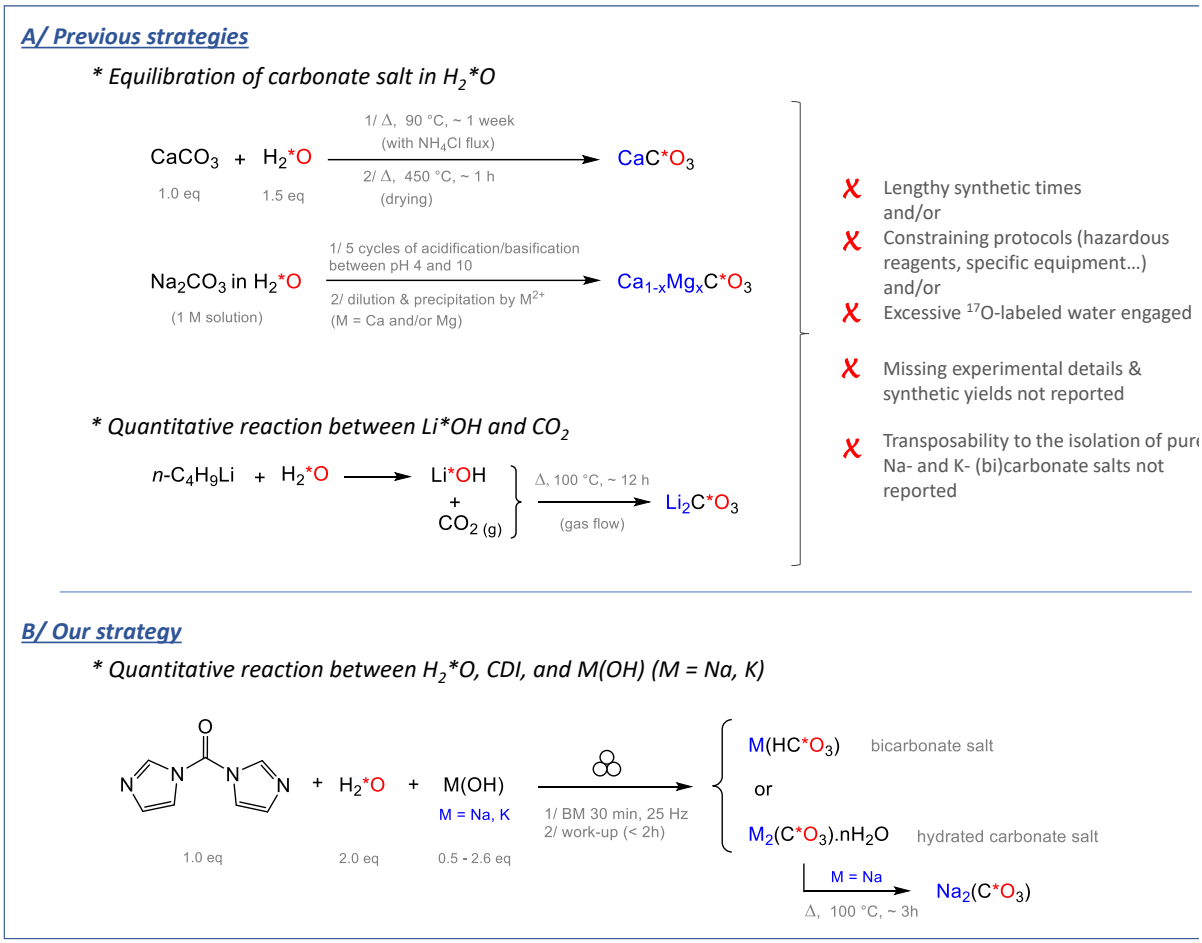

Figure 1: ^{17}O-labeling strategies for the synthesis of (bi)carbonate salts: (**A**) Examples of strategies previously described in the literature.[50-52] (**B**) CDI-based procedure proposed in the present work.

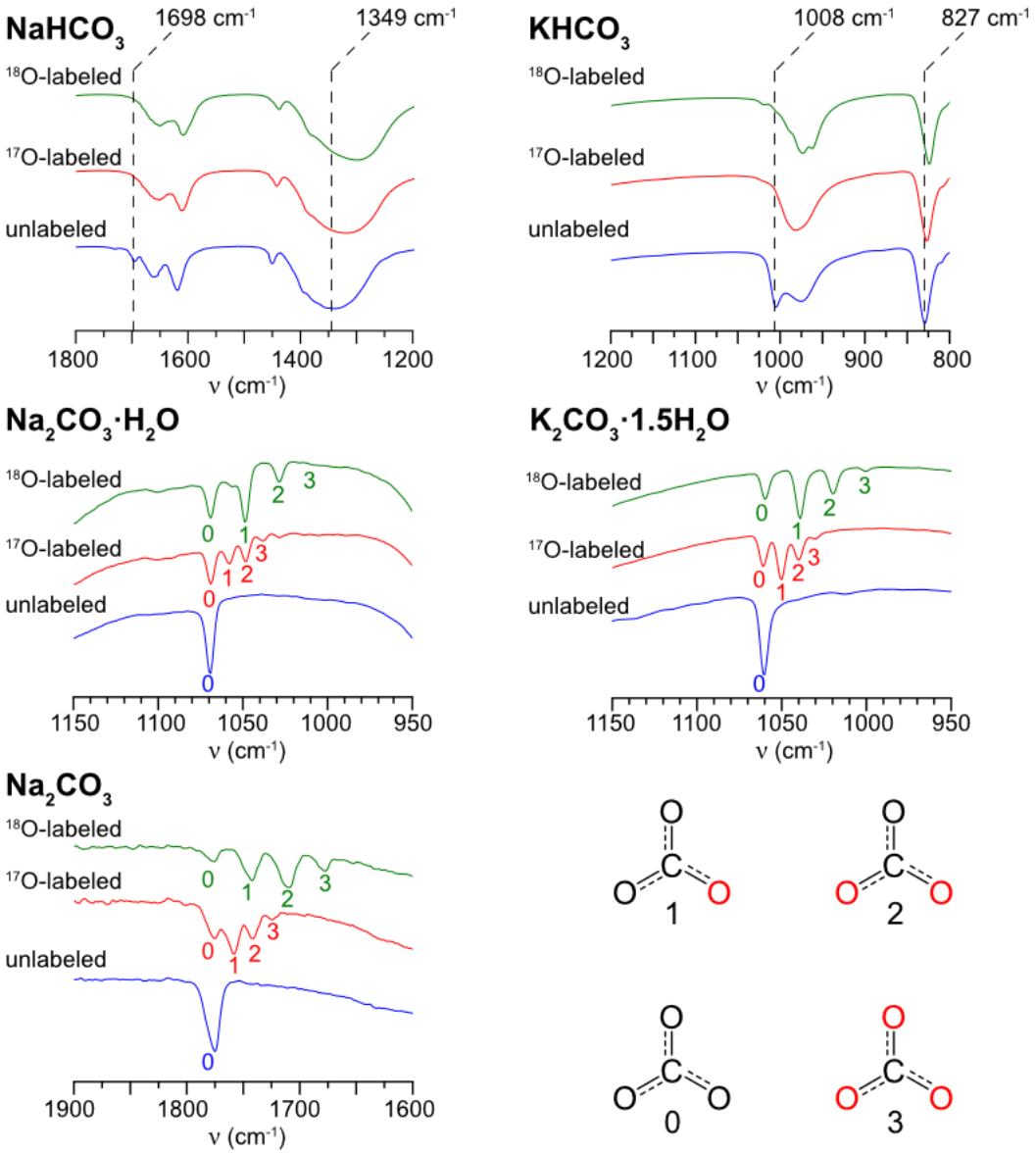

Figure 2: Experimental IR spectra, zooming into regions of interest for unlabeled (blue), ^{17}O-labeled (red), and ^{18}O-labeled Na and K (bi)carbonate salts, synthesized by mechanochemistry. The IR spectra of Na_2CO_3, $Na_2CO_3{\cdot}H_2O$, and $K_2CO_3{\cdot}1.5H_2O$ indicate the successful enrichment in ^{17}O/^{18}O by the splitting of the IR bands, due to the presence of different isotopologues in the sample (as illustrated in the bottom right corner, in which ^{17}O/^{18}O-enriched oxygens are shown in red). The dashed lines in black in the IR spectra of $NaHCO_3$ and $KHCO_3$ denote IR bands in the unlabeled purified product, which are shifted with respect to those labeled with either ^{17}O/^{18}O. The data shown here is for products which were mechanochemically enriched using $H_2{}^{18}O$ (99% ^{18}O-labeled, green spectra), or $H_2{}^{17}O$ (40% ^{17}O-labeled for $Na_2CO_3{\cdot}H_2O$ and $NaHCO_3$, and 90% ^{17}O-labeled for $KHCO_3$ and $K_2CO_3{\cdot}1.5H_2O$). The Na_2CO_3 phase analyzed here was prepared by dehydration of a monohydrate phase, for which labeling had been done by the CDI-based ball-milling procedure, using 70% ^{17}O-labeled water.

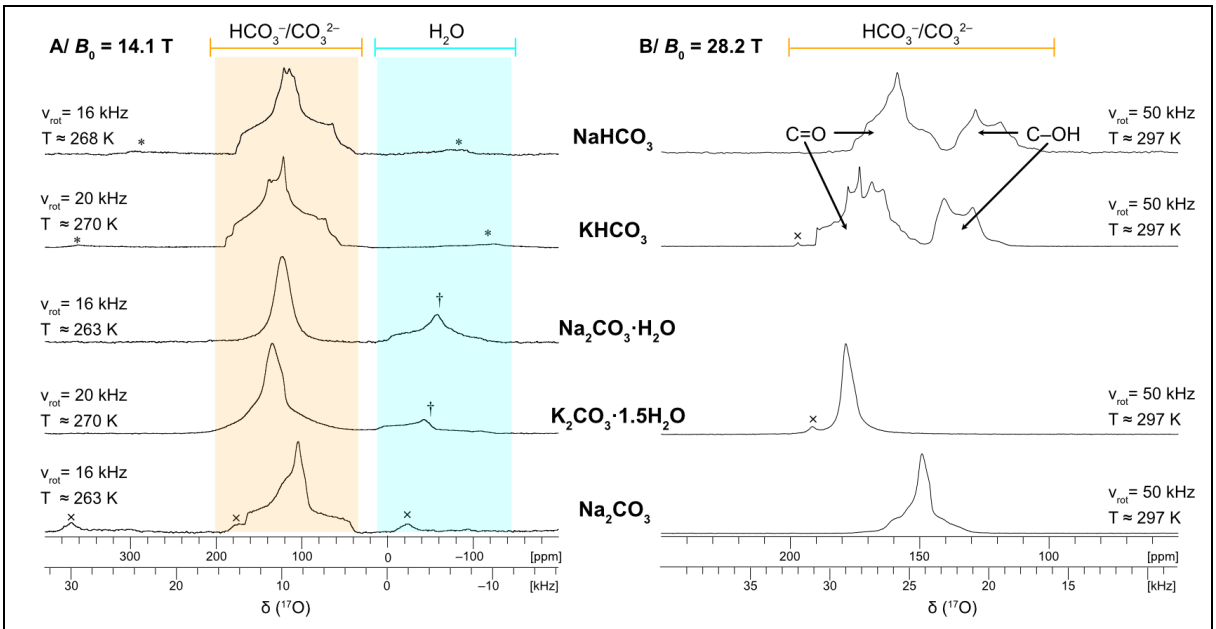

Figure 3: Experimental $^{17}O\{^{1}H\}$ MAS NMR spectra acquired at (**A**) B_0 = 14.1 T (600 MHz instrument) and (**B**) B_0 = 28.2 T (1.2 GHz instrument) on enriched bicarbonates ($NaHCO_3$ and $KHCO_3$), carbonate hydrates ($Na_2CO_3{\cdot}H_2O$ and $K_2CO_3{\cdot}1.5H_2O$), and anhydrous sodium carbonate (Na_2CO_3). Sample temperatures and spinning rates are indicated near the spectra. In (**A**), the spectral regions expected for HCO_3^-/ CO_3^{2-} (200 to 40 ppm) and crystalline H_2O (0 to –120 ppm) at 14.1 T are shown in orange and light blue, respectively. In (**B**), only the HCO_3^-/ CO_3^{2-} spectral region is shown, in which the higher resolution achieved with increasing magnetic field enables the distinction between signals arising from C=O and C–OH. Spinning sidebands are denoted with an asterisk (*), ^{17}O NMR signals arising from crystalline water with a dagger (†), and from satellite transitions with a cross (×). Further details on acquisition parameters for displayed spectra are shown in the **ESI Tables S3** and **S4**.

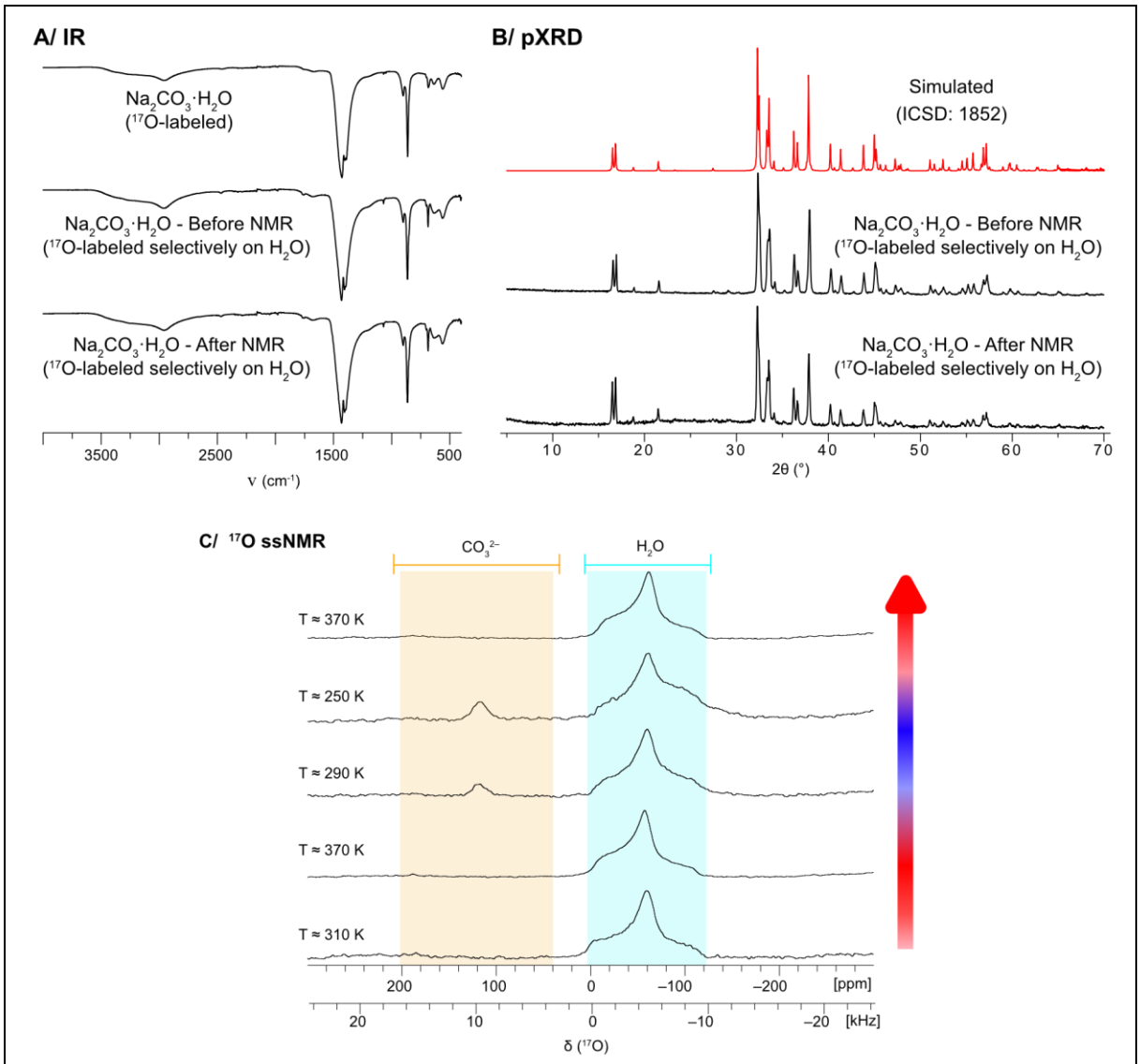

Figure 4: (**A**) Experimental IR and (**B**) pXRD (in black) of $Na_2CO_3{\cdot}H_2{}^{17}O$, before and after the *in-situ* ^{17}O ssNMR tests in (**C**), showing no observable change in its structure. The IR spectrum of the ^{17}O-labeled $Na_2CO_3{\cdot}H_2O$ (prepared by CDI hydrolysis), and the simulated X-ray diffraction pattern of $Na_2CO_3{\cdot}H_2O$ (ICSD 1852) are shown for comparison. (**C**) Experimental VT $^{17}O\{^1H\}$ MAS NMR spectra of $Na_2CO_3{\cdot}H_2O$ (selectively ^{17}O-labeled on the water) acquired at B_0 = 14.1 T (600 MHz instrument). The spectral regions for CO_3^{2-} (200 to 40 ppm) and crystalline H_2O (0 to –120 ppm) at this field are shown in orange and light blue, respectively, with sample temperatures indicated on the left for each spectrum.